Ab Initio and Molecular Dynamics Study of the Active Site of the Reaction between Ribonuclease A and Cytidyl-3′,5′-Adenosine

Anik Peeters, Ben Swerts, and Christian Van Alsenoy*

Department of Chemistry, University of Antwerp (UIA), Universiteitsplein 1, B-2610 Wilrijk, Belgium

Received: December 7, 2002; In Final Form: March 10, 2003

In this ab initio study of the reaction mechanism of ribonuclease A with cytidyl-3′,5′-adenosine, the geometry of the active site has been optimized using the Hartree−Fock method. The active site model contains the complete substrate, interacting water molecules, and fragments of eight amino acids that are involved in functional and structural interactions with the substrate. The refined conformations revealed an interesting hydrogen-bonding network that allows the prediction of the conformation of the active site in the initial step of the reaction mechanism. Based on the results of the calculations, a new mechanism is proposed: A proton is transferred from the O2′C−H2′C group to a phosphate oxygen through a water molecule. The developing charge on the phosphate group is stabilized through strong interactions with the enzyme. O2′C is hydrogen-bonded to the side chain of Lys41 as a precursor to catalysis and the two free phosphate oxygen atoms form strong hydrogen bonds with the side chain of Lys7 and the backbone of Phe120. In contrast to earlier reaction proposals, it is shown here that His12 is not directly involved in the initial step.

I. Introduction

Bovine pancreatic ribonuclease (RNase A) catalyzes the cleavage of the 3′,5′-phosphodiester linkage of RNA or nucleotide esters at the P−O5′ bond at the 3′ end of a pyrimidine in two subsequent reactions. The first reaction is a transphosphorylation to form a 2′,3′-cyclic phosphate intermediate. This cyclic nucleotide is hydrolyzed in a second reaction to yield a terminal 3′-pyrimidine nucleotide.

The interaction of RNase A with different substrates or substrate-like compounds (inhibitors), transition states, and products has been studied by X-ray or neutron diffraction,[1−12] NMR spectroscopy,[3,13−21] theoretical calculations,[22−30] and kinetic analyses.[31−41] Although most of the studies and review articles[42,43] agree that His12, His119, and Lys41 are involved in the active site of the enzyme,[42] there is no agreement on the exact mechanism in the transphosphorylation step of the reaction, and there is no straightforward evidence that His12 is essential for catalysis. In the established general acid−general base mechanism,[44,45] His12 (general base) deprotonates O2′−H2′ prior to the nucleophilic attack of O2′ on P and His119 (general acid) protonates the leaving group. Several alternatives to this mechanism have been published.[46−48] Glennon and Warshel[49] classify the different reaction proposals in two groups depending on the nature of the transition state. They used the empirical valence bond (EVB) method to compare the energetics for the two classes but were unable to resolve the controversy on the mechanism. The first group of reaction mechanisms involves a dianionic transition state (or intermediate) and includes, for example, the established general acid−general base mechanism. In the mechanism proposed by Gerlt and Gassman,[46] the dianionic phosphorane intermediate is stabilized through the formation of short, strong hydrogen bonds between the free phosphate oxygen atoms and residues Lys41, Gln11, or Phe120 of the enzyme. The second class of reaction mechanisms contains the so-called triester-like mechanisms that proceed through a monoionic transition state. In these mechanisms, one of the free phosphate oxygen atoms is protonated prior to the nucleophilic attack of O2′. Lim and Tole[47] have proposed an intraligand proton transfer of O2′ to O1P, assisted by His12. In the so-called modified Breslow mechanism[50,52−48] the first function of the acid catalyst is to protonate a free phosphate oxygen and not the leaving group. This proton transfer, however, is in conflict with the pK_a values of the different functional groups.[47]

The present study focuses on the interaction of RNase A with one of the more reactive substrates, cytidyl-3′,5′-adenosine[32] (CpA). To obtain more structural information about the first step of the transphosphorylation, a 1000 ps molecular dynamics (MD) simulation of the complete enzyme−substrate system embedded in water has been performed, followed by quantum chemical ab initio calculations for a model of the active site. Although classical MD simulations cannot simulate the initial chemical steps of the catalytic reaction, they have proved to be useful in finding productive conformations that support one or more possible mechanisms.[53] In addition to suggesting possible mechanisms, this method provides good starting structures for subsequent analysis using more elaborate techniques such as ab initio methods. Therefore, five snapshots from the MD simulation have been used to construct starting conformations for ab initio geometry optimizations. This selection of the starting structures based on the MD equilibration of the X-ray structure increases the chances to come across new mechanisms that were not previously proposed in the literature. As a third part of this study, the energy profile for the proton transfer in the initial step of the reaction mechanism has been followed for one of the optimized ab initio conformations. A detailed analysis of the results provides insight into the nature of the proton-transfer mechanism and the conformation of the transition state.

* To whom correspondence should be addressed. E-mail: alsenoy@uia.ua.ac.be. Fax: +32.3.820.23.10.

10.1021/jp027648d CCC: $25.00
Published on Web 04/19/2003

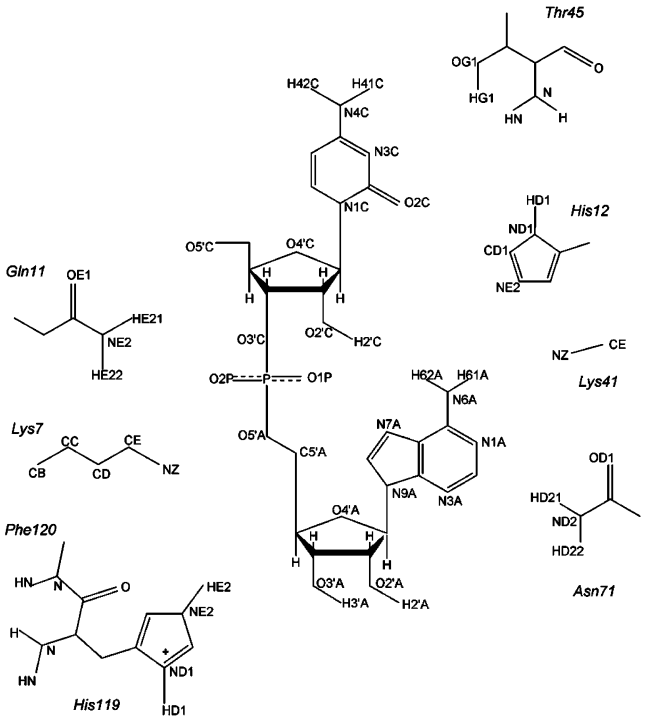

Figure 1. Schematic representation of the ab initio model system.

II. Computational Methods

A molecular dynamics simulation was performed using the molecular modeling program CHARMM,[54] starting from an X-ray structure of the complex of RNase A with deoxy-CpA (d(CpA)), an inhibitor closely related to CpA.[7] After the addition of a hydroxyl group on the C2′ atom of each ribose, the obtained enzyme/substrate complex including 164 X-ray waters was placed in a 33 Å radius sphere of TIP3P water molecules. A total of 4028 overlaid waters for which the oxygen atom was between 2.5 and 8.0 Å distant from either the protein, the substrate, or the X-ray waters were retained. The resulting system consisted of 14 496 atoms. This solvated system was subject to 200 steps of steepest descent and 1000 steps of adopted-basis Newton Raphson minimization, followed by 10 ps of heating dynamics in the presence of harmonic restraints (1 kcal/Å^2) on all enzyme and substrate atoms. This was followed by 30 of ps equilibration dynamics. Finally, 1000 ps of production dynamics were performed. Coordinates were saved every 100 fs, resulting in 10 000 sets available for further analyses. Electrostatic interactions were truncated by applying a force-switching function[55] in the region between 11 and 15 Å. van der Waals interactions were truncated at 15 Å by a shifted potential. The list of nonbonded interactions (17 Å cutoff) was updated only when necessary; the list-updating decisions were based on heuristic testing.

Five snapshots from the molecular dynamics simulation were taken as starting structures for the ab initio calculations (one snapshot taken every 200 ps: d200, d400, d600, d800, and d1000). To create a model for the active site, 171−180 atoms were extracted from these coordinates. The model includes the complete substrate (63 atoms) and 99 enzyme atoms to mimic the 8 most interesting amino acid residues: Lys7, Gln11, His12, Lys41, Thr45, Asn71, His119, and Phe120. A schematic representation and 3D image of the substrate and the enzymatic fragments involved in the model are shown in Figures 1 and 2. In Figure 1, the CHARMM-based atom numbering is only shown for the substrate and the most important enzyme atoms. In addition, three to six water molecules in close interaction

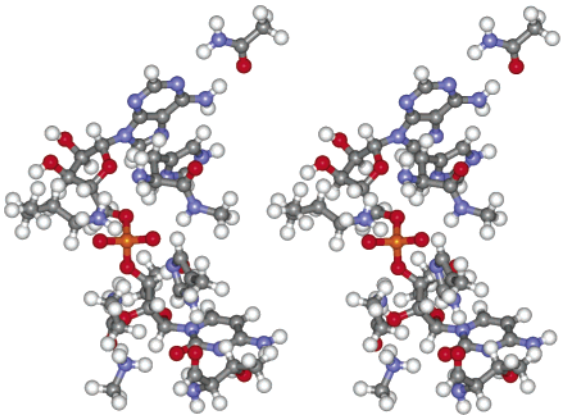

Figure 2. 3D stereo representation of the ab initio model system.

with the substrate have been included in the model. These water molecules play a crucial role in the conformation of the active site. In d200 and d800 three water molecules are included, in d400 six water molecules are optimized, and in d600 and d1000 five water molecules are involved.

All optimizations were performed with the ab initio Hartree−Fock (HF) MIA approach,[56] available in the quantum chemistry program BRABO.[57] The 6-31G basis set has been used.[58,59] During the optimizations, the relative position of the C_α representing atoms of Lys7, Gln11, and His12 and the relative orientation of their side chains were fixed by using four constraints. This was done because these three residues are part of an α-helix. For snapshot d200, it was impossible to complete the optimization even after more than 2000 steps.

For the second part of the study, the reaction coordinate R was chosen as $R = r_1 + r_2 + r_3$ with $r_1 = r$(H2′C···O(W2)), $r_2 = r$(H(W2)···O2P) and $r_3 = r$(O2′C···P). Reducing the value of R forces the proton transfer to take place (r_1 and r_2) and O2′C to move closer to P (r_3). For different values of R, the geometry has been optimized and the corresponding energy has been plotted. From these calculations, two energy profiles for the initial step in the reaction mechanism could be established. Furthermore, the combination of the three distances in the reaction coordinate allowed a detailed analysis of the nature of this reaction step: is it concerted or stepwise?

III. Results

III.1. Molecular Dynamics. In Table 1, a number of important substrate torsion angles are listed. The average values for these torsion angles during the simulation are compared to the experimental X-ray values.[7] The differences between the X-ray and MD structures can be explained by the conformational changes in the MD structure due to the addition of the O2′−H2′ hydroxyl groups. For the most important hydrogen bonds present in the enzyme−substrate system near the active site, Table 2 contains the presence throughout the simulation, the average donor−acceptor distance, and hydrogen bond angle.

The active site of the system can be subdivided into different subsites:[60] for the substrate CpA, the bases are bound to the B1 and B2 subsites, the ribose rings are found in the R1 and R2 subsites, and the phosphate group is located in the P1 subsite.

In the B1 subsite, Thr45 forms three strong hydrogen bonds with the cytidine group of the substrate (N−HN···O2C, OG1−HG1···N3C, and OG1···H41C−N4C) and one strong bond with the imidazole ring of His12 (O···HD1−ND1 (His12)). One of the water molecules in the subsite forms a very strong bond with Ser123 and was also found in the vicinity of Arg85 and the H41C atom of the substrate. Arg85 is in turn strongly

TABLE 1: Torsion Angles (in deg) of the Substrate

	expt[7]	av (rms)	d400		d600		d800		d1000	
	X-ray	MD	MD	QM	MD	QM	MD	QM	MD	QM
O4′−C1′−N1−C2	−154.8	−163 (11)	−158.9	−170.8	−151.8	−173.9	−166.8	−166.5	−177.0	−170.4
C4−N9−C1′−O4′	−103.8	−92 (13)	−81.6	−107.6	−97.1	−103.8	−91.9	−89.2	−77.3	−120.5
O5′C−C5′C−C4′C−C3′C	29.3	57 (10)	72.1	55.1	55.2	50.7	51.1	54.6	47.9	55.5
C5′C−C4′C−C3′C−O3′C	120.4	80 (7)	68.4	84.2	80.0	76.4	97.6	81.7	75.5	80.2
C4′C−C3′C−O3′C−P	−159.6	−143 (13)	−139.6	−155.8	−153.4	−161.1	−127.9	−145.4	−135.8	150.6
C3′C−O3′C−P−O5′A	56.1	81 (12)	86.8	72.3	85.5	92.9	79.4	104.5	77.8	142.2
O3′C−P−O5′A−C5′A	76.6	79 (12)	72.2	80.1	65.3	82.1	80.8	69.0	72.9	144.8
P−O5′A−C5′A−C4′A	110.3	103 (16)	96.6	95.1	125.2	101.8	89.7	107.1	110.3	71.5
O5′A−C5′A−C4′A−C3′A	173.4	173 (8)	169.2	−169.3	167.7	−178.0	174.7	172.4	174.8	−171.4
C5′A−C4′A−C3′A−O3′A	140.8	137 (12)	136.3	134.9	141.6	154.4	138.0	154.6	144.6	115.9

TABLE 2: Hydrogen Bonds Present in the MD Simulation

X−H···Y			presence (%)	X···Y (Å)	X−H···Y (deg)
(CpA)	O2′C−H2′C···O3′C	(CpA)	83	2.75	117
(CpA)	O2′C−H2′C···O1P	(CpA)	16	2.96	147
(CpA)	O2′C−H2′C···OE1	(Gln11)	16	3.21	114
(CpA)	O2′C−H2′C···NE2	(His12)	14	3.24	129
(CpA)	N4C−H41C···OG1	(Thr45)	83	3.16	138
(CpA)	N6A−H61A···OD1	(Asn71)	95	2.97	163
(Lys7)	NZ−HZ···O2P	(CpA)	94	2.71	160
(Gln11)	NE2−HE21···O2P	(CpA)	68	3.17	153
(Gln11)	N−HN···O	(Lys7)	100	2.82	164
(Gln11)	NE2−HE22···NE2	(His12)	89	3.08	158
(His12)	N−HN···O	(Phe8)	100	2.95	158
(His12)	ND1−HD1···O	(Thr45)	100	2.85	161
(Lys41)	NZ−HZ···O2′C	(CpA)	100	2.84	156
(Thr45)	N−HN···O2C	(CpA)	98	3.00	151
(Thr45)	OG1−HG1···N3C	(CpA)	100	2.88	155
(Asn71)	ND2−HD21···N1A	(CpA)	97	3.07	162
(His119)	ND1−HD1···O5′A	(CpA)	100	2.86	160
(Phe120)	N−HN···O1P	(CpA)	87	2.86	164

hydrogen bonded with Asp83, a residue that is often associated with the B1 site.[38]

The conformation of the cytidine ribose ring found in the R1 subsite is unstable during the MD trajectory. The ring takes up the C2′exo, C3′endo, C4′exo, and the O4′endo conformation. The average pseudorotation angle,[61] 34.4°, describes a twist conformation between C3′endo and C4′exo.

One of the strongest and most stable hydrogen bonds formed in the active site is the bond between O2′C and the NH_3 group of Lys41. Throughout the complete simulation, the O2′C···HZ distance is only 1.8 Å and the O2′C···HZ−NZ bond angle is approximately 25° from linearity. The hydrogen-donating character of O2′C−H2′C is more complicated. Weak hydrogen bonds are formed with O1P, Gln11, or His12 during approximately 15% of the simulation time. During the rest of the MD trajectory, an intramolecular O2′C−H2′C···O3′C hydrogen bond is formed that is in conflict with the proposed reaction mechanisms. The NE2 acceptor atom of His12 is involved in a strong bond with the side chain of Gln11 during the major part of the simulation. Other hydrogen bonds between His12 and the backbone of Phe8 and Thr45 suggest a more structural role for His12. Gln11 can be regarded as a bridging residue between the R1 subsite and the phosphate binding site, making hydrogen bonds with O2′C, O2P, His12, and Lys7. Lys7 is in turn strongly interacting with O2P.

For the study of the catalytic mechanism the phosphate binding site (**P1**) is the most interesting subsite of the enzyme. The phosphodiester torsions about the O3′C−P and P−O5′A bonds are both in the gauche region, having average values of, respectively, 81° and 79°, in close agreement with the X-ray values (56° and 77°, respectively). The free phosphate oxygen atoms, O1P and O2P, form strong hydrogen bonds with the enzyme. O1P forms also an intramolecular bond with O2′C−H2′C in the beginning of the simulation but forms a stronger hydrogen bond with the backbone of Phe120 later. O2P is hydrogen-bonded to Lys7. His119 interacts with O5′A, facilitating protonation of the leaving group.

The downstream adenine ribose in the R2 subsite prefers a slightly twisted C2′endo conformation during the complete simulation, resulting in an average pseudorotation angle P of 150.6°. In analogy with the cytidine sugar ring, a weak O2′−H2′···O3′ intramolecular hydrogen bond was present and O2′A−H2′A is involved in several short interactions with water molecules.

In the second base binding site, B2, the strong hydrogen bonds observed between Asn71 and the purine group at position N1 and N6 (OD1···H61A−N6A and ND2−HD21···N1A) suggest a significant influence on the catalytic activity. During the simulation, also van der Waals contacts were observed between the adenine base and Asn67 and Gln69. In the B2 region of the enzyme, some very strong intramolecular interactions are observed in the enzyme. The backbones of Cys65 and Gln69 are hydrogen-bonded, and also Asn71 and Cys110 are connected through two hydrogen-bond interactions.

A number of water molecules in the structure are in close contact with the enzyme (Lys7, Gln11, Arg39, Lys41, Asn67, Arg85, His119, Phe120, and Ser123) or with the substrate (O2′C−H2′C, N4C−H41C, N4C−H42C, O2′A-H2′A, and N6A−H62A). The strongest interaction with water is observed for N6A−H62A.

III.2. Ab Initio Geometry Optimization. Four ab initio geometry optimizations have been completed. The starting structures for these calculations have been derived from MD snapshots according to the procedure described in section II. In Table 1, the torsion angles of the substrate in the different snapshots (d400, d600, d800, and d1000) are shown before and after the ab initio optimizations. The values before the optimization correspond to the conformation of the MD snapshot. The largest changes in the backbone torsion angles of the substrate are observed for snapshot d1000. The torsions around P−O3′C and P−O5′A change by approximately 70° from a gauche conformation in the MD structure to a trans conformation in the ab initio optimized structure. For the other three snapshots (d400, d600, and d800), the difference between the optimized conformations of the substrate is small and there is a good agreement with the average structure obtained from the MD simulation.

In Table 3, the shortest hydrogen-bond interactions present in the optimized structures are shown. Completely in agreement with the observations for the substrate conformation, also the hydrogen-bonding network observed after optimization of d400, d600, and d800 is very similar. In d1000, a few slightly different interactions are present or important interactions are missing.

TABLE 3: Donor-acceptor Distances (in Å) for the Hydrogen Bonds: Average Value over the MD Simulation and Optimized Values for the ab Initio Active Site Conformations

X−H···Y			MD	d400	d600	d800	d1000
(CpA)	O2′C−H2′C···O1P	(CpA)	2.96				
(CpA)	O2′C−H2′C···O	(W2)			2.737	2.721	
(CpA)	O2′C−H2′C···OE1	(Gln11)	3.21				2.701
(CpA)	N6A−H61A···OD1	(Asn71)	2.97	2.788	2.783	2.785	2.778
(Lys7)	NZ−HZ1···O2P	(CpA)	2.71	2.822	2.756	2.795	2.799
(Lys7)	NZ−HZ2···O	(W3)		2.705	2.679	2.657	
(Lys7)	NZ−HZ3···O	(W4)		2.819	2.950		
(His12)	ND1−HD1···O	(Thr45)	2.85	2.909	2.892	2.865	2.906
(Lys41)	NZ−HZ1···OE1	(Gln11)		2.653	2.672	2.689	
(Lys41)	NZ−HZ2···O2C	(CpA)		2.752	2.775	2.767	
(Lys41)	NZ−HZ3···O2′C	(CpA)	2.84	2.976	2.889	2.908	
(Thr45)	OG1−HG1···N3C	(CpA)	2.88	2.809	2.805	2.800	2.789
(Asn71)	ND2−HD21···N1A	(CpA)	3.07	3.173	3.178	3.198	3.204
(His119)	ND1−HD1···O5′A	(CpA)	2.86	3.005	2.993	2.956	
(His119)	ND1−HD1···O4′A	(CpA)	3.18				2.938
(Phe120)	N−HN···O1P	(CpA)	2.86	2.966	2.946	3.070	2.963
(W2)	O−H···O2P	(CpA)		2.709	2.673	2.648	2.601
(W3)	O−H···O1P	(CpA)		2.790	2.854	2.869	2.737
(W3)	O−H···NE2	(His12)		2.719	2.698	2.669	2.685

In the B1 subsite, the hydrogen-bond interaction between OG1−HG1 (Thr45) and atom N3C of the cytidine group is omnipresent in the optimized snapshots. The backbone of Thr45 is involved in a hydrogen bond with the imidazole ring of His12. In d400, d600, and d800, O2C forms a strong interaction with one of the protons of the NH_3 group of Lys41.

The pseudorotation angle of the ribose ring present in the R1 subsite describes a C3′endo conformation in all snapshots. O2′C forms a hydrogen bond to the NH_3 group of Lys41 in three of the four snapshots, but this important interaction is not present in d1000. In d600 and d800, O2′C−H2′C forms a hydrogen bond to a water molecule (W2), which is in turn donating a hydrogen bond to the free phosphate oxygen O2P. In d1000, H2′C is hydrogen-bonded to the carbonyl oxygen OE1 of residue Gln11. His12 is not involved in a hydrogen bond with H2′C but forms an indirect hydrogen bond to O1P through a water molecule (W3).

In all optimized structures, the phosphate oxygen atoms in the P1 subsite, O1P and O2P, interact with a water molecule and a residue from the enzyme. O1P interacts with the backbone N−H of Phe120 and with water W3. The second proton of this water molecule forms a strong bond with NE2 of His12, while the oxygen atom is accepting a hydrogen bond from the NH_3 group of Lys7. O2P forms a hydrogen bond with another hydrogen atom of the NH_3 group of Lys7 and with water molecule W2. W2 accepts a hydrogen bond from H2′C in d600 and d800 and from H3T in d400. In d600 and d800, this water molecule could thus mediate the proton transfer between O2′C and O2P. Protonation of the leaving group is facilitated in d400, d600, and d800 through a strong interaction between His119 and O5′A. This hydrogen bond is absent in d1000.

In the R2 subsite, the adenine ribose ring exists in C2′endo conformation in d600 and d800, C1′exo in d1000, and an intermediate conformation in d400.

Asn71 is the only B2 subsite residue involved in the ab initio model. It forms a strong hydrogen bond with N6A−H61A.

Only a limited number of water molecules (between three and six) have been included in the ab initio model calculations. These water molecules form a bridge between H2′C and O2P or between O1P and His12. Other molecules interact with Lys7, Gln11, Lys41, His119, O5′C−H5T, O3′A-H3T, O3′A, O4′C, O5′C, and N7A.

III.3. Ab Initio Reaction Coordinate. Following the ab initio geometry optimizations, the first part of the transphosphorylation step in the reaction mechanism has been followed for one of the optimized snapshots (d800). On the basis of the optimized conformation (section III.2), the attack of O2′C on the phosphor atom is expected to be preceded or accompanied by the transfer of H2′C to a phosphate oxygen (O2P) through a water molecule. Therefore, the reaction coordinate *R* has been chosen as the sum of three distances: H2′C···O(W2) (r_1), H1(W2)···O2P (r_2), and O2′C···P (r_3), indicated in Figure 3. At the start of the reaction, the value for this reaction coordinate is 7.48 Å ($r_1 = 1.755$, $r_2 = 1.686$, and $r_3 = 4.039$ Å). The reaction coordinate has been varied between 7.0 and 3.7 Å.

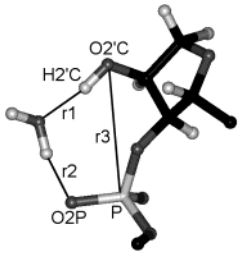

Figure 3. Intra- and intermolecular distances used to construct the reaction coordinate *R*.

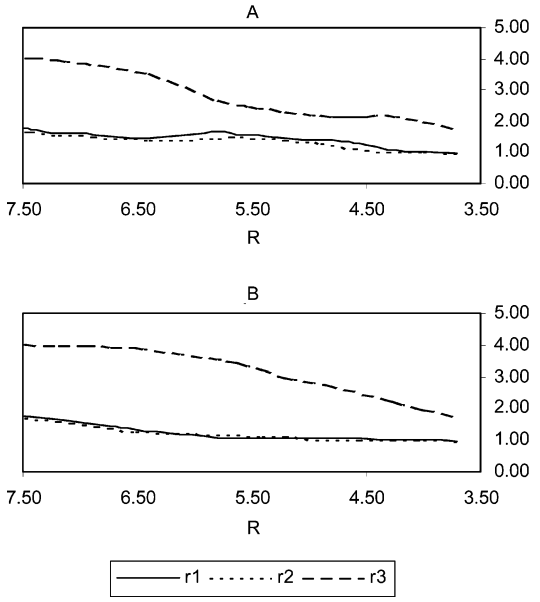

Figure 4. Evolution of individual r_1, r_2, and r_3 distances (in Å) along reaction coordinate *R*.

For the two reaction mechanisms that have been studied, the values of r_1, r_2, and r_3 are plotted in Figure 4A,B. In the first (concerted) reaction mechanism (Figure 4A), O2′C first approaches P until it reaches a distance of approximately 2.2 Å, followed by the concerted proton transfer along r_1 and r_2 and the final attack of O2′C on P. In the second (stepwise) mechanism (Figure 4B), the proton-transfer precedes the nucleophilic attack.

For the points calculated along these reaction pathways, the energy has been plotted in Figure 5. The solid curve corresponds to the first (concerted) mechanism, while the dotted line describes the energy along the second (stepwise) mechanism. According to the calculations, the energy difference between the initial and final products of the first step in the reaction mechanism is 6.25 kcal/mol, whereas the activation energy is 24.6 and 31.6 kcal/mol for the concerted and stepwise mechanism, respectively.

Along the reaction coordinate of the concerted mechanism, the changes of the geometrical parameters such as the bond

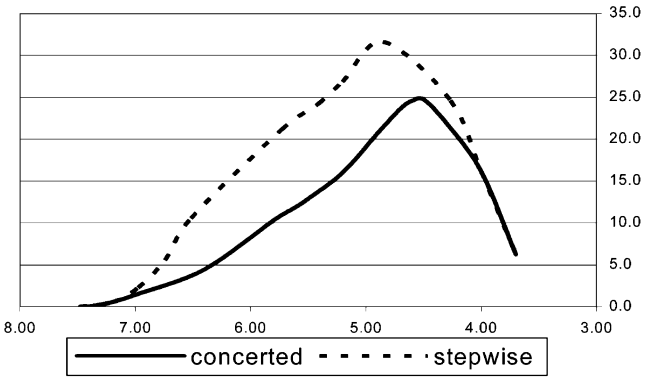

Figure 5. Energy (in kcal/mol) along concerted and stepwise reaction pathway.

lengths and angles of the substrate and the interactions with the enzyme have been followed. In the first point along the reaction coordinate, the H1−O−H2 angle for the water molecule W2 involved in the reaction is 113.0°, and H2′C is coordinated along one of the lone pairs of the water oxygen atom (H2′C−O(W2)−H2(W2) = 118.7°). After the concerted O2′C···H2′C3′···O(W2), and O(W2)···H1(W2)···O2P proton transfers, the H2′C−O(W2)−H2(W2) angle is 112.8° and the original water angle H1−O−H2 is very large, 137.2°. After the transfer, H2′C and H1(W2) stay within hydrogen-bonding distance from their respective original donor atoms.

The P−O2P bond changes from a partial double bond (1.591 Å) in point 1 (R = 7.48 Å) to a hydroxyl bond (1.697 Å) in point 16 (R = 3.70 Å). P−O1P, on the other hand, does not change significantly (1.577−1.595 Å) throughout the first reaction step.

At the start of the reaction, P is connected to four oxygen atoms (O3′C, O1P, O2P, and O5′A) arranged in a tetrahedron and O2′C moves in from an angle that is not ideal (O2′C−P−O3′C = 31.3°). During the reaction, the coordination around P changes into a trigonal bipyramid with the incoming (O2′C) and leaving (O5′A) groups in axial positions. The angles between the equatorial oxygen atoms change to approximately 120° during the reaction.

The P−O5′A bond length increases as O2′C moves in to attack P. Simultaneously the distance between O5′A and His119 (HD1 atom) decreases from 1.953 Å in point 1 to 1.747 Å in point 16. The N−H distance (ND1−HD1) in His119 also increases slightly (from 1.016 to 1.032 Å).

The hydrogen bond between Lys41 and O2′C is broken during the reaction, but the interactions of Lys41 with Gln11 and with the pyrimidine ring of the substrate remain strong.

IV. Discussion

IV.1. Static Picture before the Reaction. Based on the results of the MD simulation and the ab initio geometry optimizations and information obtained from the literature, a picture of the active site at the start of the reaction has been developed. The hydrogen bonds present in the calculated structures (Tables 2 and 3) are responsible for obtaining a good alignment between the substrate and the enzyme or are directly involved in the catalytic reaction.

The primary base binding subsite, B1, binds only pyrimidine nucleotides and demonstrates an approximate 30-fold preference for cytidine versus uridine.[38] This specificity is mediated by the most important residue in this site, Thr45, which is conserved in all 41 amino acid sequences of pancreatic ribonucleases studied by Beintema et al.[62] The importance of Thr45 is confirmed in our MD simulation, in which this residue forms three strong hydrogen bonds with the cytidine group of the substrate (N−HN···O2C, OG1−HG1···N3C, and OG1···H41C−N4C). In a MD simulation of the RNase A/UpA system,[28] only the equivalent of the first hydrogen bond (N−HN···O2U) was observed and the two remaining hydrogen contacts were replaced by slightly weaker interactions with Thr45 and Ser123, explaining the preference of cytidine over uridine in RNase A.[38]

The geometry optimizations confirmed the conformation of the ribose ring in the R1 subsite to be C3′endo, one of the two preferred conformations (C2′endo and C3′endo) for the sugar pucker in nucleotides.[63] In a previous study of the isolated substrate CpA,[64] the C3′endo conformation was also observed. In a short simulation of CpA with RNase A by Haydock et al.,[23] the ribose ring adopted a conformation corresponding to a pseudorotation angle of 34°, in excellent agreement with our MD results (34.4°). Throughout another simulation,[28] the uridine ribose of UpA also remains at C3′endo. In Zegers' crystal structure of d(CpA) complexed with RNase A, both deoxyriboses take up the C2′endo conformation.[61]

The importance of Lys41, as already indicated by Walter and Wold[31]and emphasized in later studies,[7,14,33,37] has been confirmed in the present study. The strong hydrogen bond between Lys41 and O2′C shown in Table 3 was first proposed in a theoretical study by Haydock et al.[23] Different experiments[2,3,37] have also shown the presence of this interaction in the transition state of the reaction.

One of the key issues in the reaction mechanism is the hydrogen-bond-donating character of O2′C−H2′C. According to the present calculations, O2′C−H2′C is in contact with a free phosphate oxygen atom through a water molecule and it is not involved in an interaction with His12. This conformation suggests an intramolecular proton transfer at the start of the reaction, similar to the mechanism proposed by Lim et al.[47] Glennon and Warshel also considered this possibility in their empirical valence bond study.[49] His12 is not directly involved in the reaction but forms strong hydrogen bonds with the side chains of Gln11, the backbone of Phe8 and Thr45, and a water molecule, indicating a more structural role for His12. This is in agreement with a study by Gutte,[65] who concluded that a synthetic 63-residue RNase A analogue lacking His12 exhibits full RNase A activity.[65] Thompson and Raines[66] reported a 10^4-fold decrease in k_{cat}/K_m for the H12A mutant with respect to the wild type. However, this might also be caused by geometrical changes in the active site of the mutant due to the elimination of the side chain of His12 and its important structural hydrogen bond with Thr45. In addition, a number of studies[2,3] indicate that, in contrast to what is expected on the basis of the established mechanism, in the transition state His12 interacts with an equatorial phosphate oxygen instead of the apical O2′C. In the present study, this interaction with an equatorial phosphate oxygen is mediated through a water molecule (W3). The role of His12 as a base has also been studied by Dantzman,[67] but the poor catalysis for the cleavage of 2′-deoxy-2′-thio-UpA compared to UpA could not be explained.[42]

In the model proposed on the basis of the present calculations, the phosphodiester torsions about the O3′C−P and P−O5′A bonds in the P1 subsite are both in the gauche region, in close agreement with the X-ray values (55° and 77°, respectively). When model calculations were performed[68] with two nucleosides attached to the phosphate group and the ribose fragments placed in the C3′endo geometry, energy minima were found in the (−g,−g) and (+g,+g) regions. The fully extended (t,t) conformation is energetically unfavorable owing to the gauche or

anomeric effect of the lone-pair orbitals on the backbone ester oxygen atoms O3′ and O5′.[68,69] Some authors report the (−g,−g) conformer to have a lower energy, but strong hydrogen bonds between the substrate and the enzyme suggest that the (+g,+g) conformation found here interacts very well with the enzyme. Most of the conformations obtained by Seshadri et al. were close to (+g,−g), although in a few cases also (+g,+g) and (t,+g) was observed.[26]

Both free phosphate oxygen atoms are involved in two strong hydrogen bonds. O1P is connected to His12 through a water molecule and forms a second hydrogen bond with the backbone of Phe120. O2P forms an indirect hydrogen bond with O2′C−H2′C through a water molecule and a second one with Lys7. The importance of Lys7 is emphasized by the fact that this residue also forms an indirect hydrogen bond (through a water molecule) to O1P. The O1P···H−N (Phe120) interaction has also been observed in the MD simulations of RNase A/UpA by Seshadri et al.[28] The existence of the hydrogen bonds with Lys7 and Phe120 has been confirmed by X-ray diffraction,[1,70] neutron diffraction, and NMR spectroscopy.[3] However, in some experimental studies, Lys7 is assigned to the P2 binding site.[39,40] This is in conflict with the strong interaction observed throughout the complete MD simulation of the complex of RNase A with CpA.

His119 interacts with O5′A, facilitating protonation of the leaving group. In some other studies, this histidine molecule was expected to interact with one of the free phosphate oxygen atoms.[2] According to our results, His119 is also involved in structural interactions. The backbone forms two strong hydrogen bonds with Ala109, whereas the side chain is connected to Asp121. Because His119 plays a structural, as well as a mechanistic, role, it is one of the most important residues in the RNase A enzyme. This importance has been emphasized in mutagenesis studies.[66,71]

The base present in the R2 subsite is in the C2′endo conformation. Seshadri et al.[28] argued in a MD study of the complex of RNase A with UpA that this conformation guarantees a stable interaction of the substrate with Asn71 in the B2 site.

When adenine is placed in the second base binding site, B2, the relative saturation rate for cleavage of the dinucleotide CpX is larger than that for any other base at B2, indicating that the interactions at the B2 subsite are important for the reaction mechanism.[72] Site-directed mutagenesis of amino acids in the B2 subsite indicates that Gln69 is not involved in productive interactions with any of the dinucleotides studied (CpA, CpC, CpG, CpU). Asn71, on the other hand, is an important component of the B2 subsite.[34] Glu111 is only involved if the nucleotide in the B2 site is guanosine, suggesting that a productive base-selective interaction exists between Glu111 and a guanosine ring. According to an energy minimization study of the RNase A/UpA system,[26] Gln69 and Glu111 form hydrogen bonds with the adenosine base in a 4′endo conformation, whereas in MD simulations,[28] the ribose adopts a C2′endo conformation, resulting in very strong hydrogen bonds with Asn71. The latter were also observed in the d(CpA)−RNase A X-ray structure by Zegers and co-workers.[7] The hydrogen bonds observed between Asn71 and the leaving group at position N1 and N6 (OD1···H61A−N6A and ND2−HD21···N1A) suggest a significant influence on the catalytic activity. During the simulation, weaker van der Waals contacts were observed between the adenine base and Asn67 and Gln69.

The present MD simulation and ab initio geometry optimizations point out the role of the water molecules in the reaction mechanism. One water molecule forms the bridging gap between O2′C−H2′C and the phosphate oxygen O2P. A second important water molecule forms a bridge between O1P and His12. Other water molecules assist in completing the network that ensures a proper alignment of the substrate with the enzyme in the active site.

IV.2. Reaction Mechanism. Based on the results of the MD simulation and the ab initio geometry optimizations, a starting structure and reaction mechanism for the reaction have been proposed in section IV.1. Subsequently, the structural and energetic changes with the reaction coordinate chosen for this new mechanism have been studied. It should be noted, however, that in this work only the initial step in the transphosphorylation has been studied. Because of the limited size of the model system used, it was impossible to follow the reaction until the cyclic phosphorane intermediate was formed. In the final structure obtained in this study, the attack of O2′C on the phosphor atom is completed, but the P−O5′A bond is not broken.

According to the calculated reaction barriers (section III.3), the reaction is likely to proceed through a concerted double proton transfer of H2′C to water (W2) and H(W2) to O2P and nucleophilic attack of O2′C on P. The monoionic intermediate formed in this way is stabilized through strong hydrogen bonds that were in most cases already present at the start of the reaction. The hydrogen bond between His119 and the O5′A of the leaving group is 0.02 Å shorter and more linear than that at the start of the reaction. The interaction of Lys7 with O2P is weaker because this oxygen atom is now a hydroxyl oxygen. The interactions of O1P with water W3 and the backbone of Phe120, on the other hand, are significantly stronger. Lys41 strengthens its interaction with the pyrimidine ring (O2C) after the loss of its strong hydrogen bond with O2′C. The second hydrogen bond of the Lys41 NH_3 group with Gln11 is slightly weaker in the intermediate because Gln11 is involved in a new hydrogen bond with water W2. This hydrogen bond again emphasizes the role of this catalytic water. Lys7, Gln11, Lys41, and His119 are the most important amino acids involved in the reaction.

During the past decade, a number of theoretical studies have addressed the RNase A reaction mechanism, using small model systems to complete enzyme−substrate complexes. Lim and Tole[47] studied 2-hydroxyethyl methyl phosphate as a model for the reaction in RNase A using HF/3-21+G* geometry optimizations. They calculated an activation free energy of 35.4 kcal/mol and observed a monoionic phosphorane intermediate 30.9 kcal/mol less stable than the reactant. The results obtained here for a larger model system including amino acid mimics also indicate the presence of a monoionic intermediate.

Wladkowski et al.[73] also used HF/3-21+G* calculations but extended Lim's "substrate only" model with methyleneimines and methylamine to mimic the histidine (His12 and His119) and Lys41 residues of the enzyme, respectively. The reaction barrier (13.7 kcal/mol) and the relative energy of the monoionic phosphorane structure (+5.4 kcal/mol) obtained by these authors are significantly smaller than the results presented by Lim and Tole. This is mainly due to a stabilization of the transition states and intermediates through electrostatic and hydrogen-bonding interactions with the amino acid mimics included in the larger model.

In one of the most recent model calculations, performed by Vishveshwara et al.,[74] the intermolecular proton transfer from O2′−H2′ to His12, accompanied by a simultaneous transfer of a proton from Lys41 to O2′C, has been studied. The authors

used a model including methanol, methylamine, and imidazole to mimic O2′−H2′, Lys41, and His12, respectively. With this limited model, the attack of O2′C on phosphor could not be studied. When MP2/6-31+G** was used, the reaction barrier for proton transfer was less than 2 kcal/mol, and for the DFT-(B3LYP)/6-31+G**, the barrier was even lower (1.07 kcal/mol).

In 1998, Glennon and Warshel[49] studied a model containing the complete enzyme/substrate system and calculated the catalytic effect of the enzyme using the empirical valence bond method. The authors compared the transphosphorylation reactions with a dianionic and monoionic intermediate and observed in both cases an activation free energy of approximately 22 kcal/mol. The dianionic cyclic phosphorane intermediate was slightly more stable than the monoionic intermediate. The value obtained by Glennon and Warshel for the monoionic intermediate is in good agreement with the activation energy obtained in the present study.

Although in the literature no direct experimental information is available with which to compare the present results, a number of studies have been performed on initial and transition-state analogues that support some of the interactions in the active site described in this paper. In a joint X-ray/neutron diffraction analysis of a transition-state analogue complex of RNase A and uridine 2′,3′-cyclic vanadate,[2] Gln11 and the backbone of Phe120 were found to interact with the nonbridging oxygen atoms. In the final structure reported here, the NH_2 group of Gln11 interacts with O1P through water W3 and Phe120 shows exactly the interaction observed in the experiment.

According to site-directed mutagenesis by Panov et al.,[71] the role of His119 is not restricted to protonation of the leaving group alone but the histidine residue also participates in stabilization of the transition state. Although no direct interaction with the free phosphate oxygen atoms was observed here, the strengthening of the hydrogen bond between His119 and Lys7 supports the involvement of His119 through an indirect link with O2P and water W3.

In a review article, Raines[42] raised some questions about the role of His12 in catalysis due to the lack of straightforward experimental evidence. He also discussed the possibility of using a water molecule as a base and argued that water would not be a good candidate to replace His12 because of the decrease in k_{cat} observed for the H12A mutant.[66] However, this decrease could also be caused by the loss of important structural hydrogen bonds, for example, the hydrogen bond with the backbone of Thr45, a residue responsible for the pyrimidine specificity of the enzyme. The water molecule present in this study does not act as a base because it is passing a hydrogen atom from O2′C to O2P.

V. Conclusions

In this paper, the geometry and the reaction mechanism in the active site of the complex of ribonuclease A with cytidyl-3′,5′-adenosine have been studied using molecular dynamics and ab initio Hartree−Fock methods. The model used for the quantum chemical calculations contains the complete substrate, interacting water molecules, and fragments of eight amino acids that are involved in functional and structural interactions with the substrate. The geometry and intermolecular interactions of the refined conformations have been evaluated, and an interesting hydrogen-bonding network has been revealed. This network allows the prediction of the conformation of the active site in the initial step of the reaction mechanism. Based on the results of the calculations, a new mechanism is proposed: A proton is transferred from the O2′C−H2′C group to a phosphate oxygen through a water molecule. The phosphate group is stabilized through strong interactions with the side chain of Lys7 and the backbone of Phe120. O2′C is hydrogen-bonded to the side chain of Lys41 as a precursor to catalysis. In the optimized conformations, His12 is not directly involved in the deprotonation of O2′C−H2′C but interacts with a free phosphate oxygen through a water molecule. According to the study of the reaction coordinate, the proton transfer and the nucleophilic attack take place simultaneously and the activation energy is approximately 25 kcal/mol.

In this study, we proposed a new mechanism for the initial step of the transphosphorylation in the reaction between ribonuclease A and cytidyl-3′,5′-adenosine. The mechanism is based on a molecular dynamics simulation and quantum chemical calculations for a moderately sized model system. Preliminary calculations following the reaction coordinate indicate that the activation barrier is approximately 25 kcal/mol. To obtain a more reliable estimate of the energetics of the whole reaction mechanism, a larger model is needed, including solvation and entropic effects, preferably within a QM/MM framework.

Acknowledgment. The authors gratefully acknowledge support by the University of Antwerp under Grant GOA-BOF-UA-23. B.S. thanks the Flemish governmental institution IWT for a predoctoral grant. A.P. thanks Dr. B. R. Brooks for useful discussions on the MD simulations.

References and Notes

(1) Borkakoti, N. *Eur. J. Biochem.* **1983**, *132*, 89.
(2) Wlodawer, A.; Miller, M.; Sjolin, L. *Proc. Natl. Acad. Sci. U.S.A.* **1983**, *80*, 3628.
(3) Borah, B.; Chen, C. W.; Egan, W.; Miller, M.; Wlodawer, A.; Cohen, J. S. *Biochemistry* **1985**, *24*, 2058.
(4) McPherson, A.; Brayer, G.; Cascio, D.; Williams, R. *Science* **1986**, *232*, 765.
(5) Nachman, J.; Miller, M.; Gilliland, G. L.; Carty, R.; Pincus, M.; Wlodawer, A. *Biochemistry* **1990**, *29*, 928.
(6) Aguilar, C. F.; Thomas, P. J.; Moss, D. S.; Mills, A.; Palmer, R. A. *Biochim. Biophys. Acta* **1991**, *1118*, 6.
(7) Zegers, I.; Maes, D.; Daothi, M. H.; Poortmans, F.; Palmer, R.; Wyns, L. *Protein Sci.* **1994**, *3*, 2322.
(8) Fontecilla-Camps, J. C.; de Llorens, R.; le Du, M. H.; Cuchillo, C. M. *J. Biol. Chem.* **1994**, *269*, 21526.
(9) Leonidas, D. D.; Shapiro, R.; Irons, L. I.; Russo, N.; Acharya, K. R. *Biochemistry* **1997**, *36*, 5578.
(10) Vitagliano, L.; Merlino, A.; Zagari, A.; Mazzarella, L. *Protein Sci.* **2000**, *9*, 1217−1225.
(11) Chatani, E.; Hayashi, R.; Moriyama, H.; Ueki, T. *Protein Sci.* **2002**, *11*, 72−81.
(12) Berisio, R.; Sica, F.; Lamzin, V. S.; Wilson, K. S.; Zagari, A.; Mazzarella, L. *Acta Crystallogr., Sect. D: Biol. Crystallogr.* **2002**, *58*, 441−450.
(13) Gorenste, Dg.; Wyrwicz, A. *Biochem. Biophys. Res. Commun.* **1973**, *54*, 976.
(14) Jentoft, J. E.; Gerken, T. A.; Jentoft, N.; Dearborn, D. G. *J. Biol. Chem.* **1981**, *256*, 231−236.
(15) Sportelli, L.; Viti, V. *Stud. Biophys.* **1984**, *99*, 35.
(16) Hahn, U.; Ruterjans, H. *Eur. J. Biochem.* **1985**, *152*, 481.
(17) Hahn, U.; Desaihahn, R.; Ruterjans, H. *Eur. J. Biochem.* **1985**, *146*, 705−712.
(18) Dobson, C. M.; Lian, L. Y. *FEBS Lett.* **1987**, *225*, 183.
(19) Alonso, J.; Paolillo, L.; Dauria, G.; Nogues, M. V.; Cuchillo, C. M. *Int. J. Pept. Protein Res.* **1988**, *31*, 537.
(20) Veenstra, T. D.; Lee, L. *Biophys. J.* **1994**, *67*, 331.
(21) Toiron, C.; Gonzalez, C.; Bruix, M.; Rico, M. *Protein Sci.* **1996**, *5*, 1633.
(22) Brunger, A. T.; Brooks, C. L.; Karplus, M. *Proc. Natl. Acad. Sci. U.S.A.* **1985**, *82*, 8458.
(23) Haydock, K.; Lim, C.; Brunger, A. T.; Karplus, M. *J. Am. Chem. Soc.* **1990**, *112*, 3826.
(24) Seshadri, K.; Balaji, P. V.; Rao, V. S. R.; Vishveshwara, S. *J. Biomol. Struct. Dyn.* **1993**, *11*, 395.

(25) Straub, J. E.; Thirumalai, D. *Proteins* **1993**, *15*, 360.
(26) Seshadri, K.; Rao, V. S. R.; Vishveshwara, S. *J. Biomol. Struct. Dyn.* **1994**, *12*, 581.
(27) Straub, J. E.; Lim, C.; Karplus, M. *J. Am. Chem. Soc.* **1994**, *116*, 2591.
(28) Seshadri, K.; Rao, V. S. R.; Vishveshwara, S. *Biophys. J.* **1995**, *69*, 2185.
(29) Nadig, G.; Vishveshwara, S. *Biopolymers* **1997**, *42*, 505.
(30) Lopez, X.; York, D. M.; Dejaegere, A.; Karplus, M. *Int. J. Quantum Chem.* **2002**, *86*, 10.
(31) Walter, B.; Wold, F. *Biochemistry* **1976**, *15*, 304.
(32) Katoh, H.; Yoshinaga, M.; Yanagita, T.; Ohgi, K.; Irie, M.; Beintema, J. J.; Meinsma, D. *Biochim. Biophys. Acta* **1986**, *873*, 367.
(33) Trautwein, K.; Holliger, P.; Stackhouse, J.; Benner, S. A. *FEBS Lett.* **1991**, *281*, 275.
(34) Tarragona-Fiol, A.; Eggelte, H. J.; Harbron, S.; Sanchez, E.; Taylorson, C. J.; Ward, J. M.; Rabin, B. R. *Protein Eng.* **1993**, *6*, 901.
(35) Herschlag, D. *J. Am. Chem. Soc.* **1994**, *116*, 11631.
(36) Delcardayre, S. B.; Raines, R. T. *Biochemistry* **1994**, *33*, 6031.
(37) Messmore, J. M.; Fuchs, D. N.; Raines, R. T. *J. Am. Chem. Soc.* **1995**, *117*, 8057.
(38) Delcardayre, S. B.; Raines, R. T. *J. Mol. Biol.* **1995**, *252*, 328.
(39) Fisher, B. M.; Ha, J. H.; Raines, R. T. *Biochemistry* **1998**, *37*, 12121.
(40) Fisher, B. M.; Schultz, L. W.; Raines, R. T. *Biochemistry* **1998**, *37*, 17386.
(41) Schultz, L. W.; Quirk, D. J.; Raines, R. T. *Biochemistry* **1998**, *37*, 8886.
(42) Raines, R. T. *Chem. Rev.* **1998**, *98*, 1045.
(43) Chatani, E.; Hayashi, R. *J. Biosci. Bioeng.* **2001**, *92*, 98−107.
(44) Richards, F. M.; Wyckoff, H. W. *The enzymes*; Academic Press: New York, 1971; Vol. 4.
(45) Blackburn, P.; Moore, S. *The enzymes*; Academic Press: New York, 1982; Vol. 15.
(46) Gerlt, J. A.; Gassman, P. G. *Biochemistry* **1993**, *32*, 11943.
(47) Lim, C.; Tole, P. *J. Am. Chem. Soc.* **1992**, *114*, 7245.
(48) Breslow, R.; Xu, R. *Proc. Natl. Acad. Sci. U.S.A.* **1993**, *90*, 1201.
(49) Glennon, T. M.; Warshel, A. *J. Am. Chem. Soc.* **1998**, *120*, 10234.
(50) Anslyn, E.; Breslow, R. *J. Am. Chem. Soc.* **1989**, *111*, 4473.
(51) Breslow, R.; Huang, D. L.; Anslyn, E. *Proc. Natl. Acad. Sci. U.S.A.* **1989**, *86*, 1746.
(52) Breslow, R.; Xu, R. *J. Am. Chem. Soc.* **1993**, *115*, 10705.
(53) Chatfield, D. C.; Brooks, B. R. *J. Am. Chem. Soc.* **1995**, *117*, 5561.
(54) Brooks, B. R.; Bruccoleri, R. E.; Olafson, B. D.; States, D. J.; Swaminathan, S.; Karplus, M. *J. Comput. Chem.* **1983**, *4*, 187.
(55) Steinbach, P. J.; Brooks, B. R. *J. Comput. Chem.* **1994**, *15*, 667−683.
(56) Van Alsenoy, C. *J. Comput. Chem.* **1988**, *9*, 620.
(57) Van Alsenoy, C.; Peeters, A. *THEOCHEM* **1993**, *105*, 19.
(58) Ditchfield, R.; Hehre, W.; Pople, J. *J. Chem. Phys.* **1971**, *54*, 724.
(59) Hehre, W.; Ditchfield, R.; Pople, J. *J. Chem. Phys.* **1972**, *56*, 2257.
(60) Pares, X.; Nogues, M. V.; Dellorens, R.; Cuchillo, C. M. *Essays Biochem.* **1991**, *26*, 89.
(61) Altona, C.; Sundaralingam, M. *J. Am. Chem. Soc.* **1972**, *94*, 8205.
(62) Beintema, J. J.; Schuller, C.; Irie, M.; Carsana, A. *Prog. Biophys. Mol. Biol.* **1988**, *51*, 165.
(63) Saenger, W. *Principles of Nucleic Acid Structure*; Springer-Verlag: New York, 1984.
(64) Peeters, A.; Van Alsenoy, C. *Biopolymers* **1999**, *50*, 697.
(65) Gutte, B. *J. Biol. Chem.* **1978**, *253*, 3837.
(66) Thompson, J. E.; Raines, R. T. *J. Am. Chem. Soc.* **1994**, *116*, 5467.
(67) Dantzman, C. L. Ph.D. Thesis, University of Wisconsin-Madison, Madison, WI, 1998.
(68) Govil, G. *Biopolymers* **1976**, *15*, 2303−2307.
(69) Srinivasan, A. R.; Yathindra, N.; Rao, V. S. R.; Prakash, S. *Biopolymers* **1980**, *19*, 165.
(70) Boque, L.; Coll, M. G.; Ribo, M.; Cuchillo, C. M.; Fita, I.; Vilanova, M. *Protein Pept. Lett.* **1998**, *5*, 101−108.
(71) Panov, K. I.; Kolbanovskaya, E. Y.; Okorokov, A. L.; Panova, T. B.; vanScheltinga, A. C. T.; Karpeisky, M. Y.; Beintema, J. J. *FEBS Lett.* **1996**, *398*, 57.
(72) Witzel, H.; Barnard, E. A. *Biochem. Biophys. Res. Commun.* **1962**, *7*, 295.
(73) Wladkowski, B. D.; Krauss, M.; Stevens, W. J. *J. Phys. Chem.* **1995**, *99*, 6273.
(74) Vishveshwara, S.; Madhusudhan, M. S.; Maizel, J. V. *Biophys. Chem.* **2001**, *89*, 105.